THE JOURNAL OF PHYSICAL CHEMISTRY A
A JOURNAL OF THE AMERICAN CHEMICAL SOCIETY

pubs.acs.org/JPCA Article

Triangular Cd(II)−Sm(III) Schiff Base Complex with Dual Visible and Near-Infrared Luminescent Responses to Nitro Explosives

Mengyu Niu, Xiaoping Yang,* Yanan Ma, Dongliang Shi, and Desmond Schipper

Cite This: *J. Phys. Chem. A* 2021, 125, 251−257 Read Online

ABSTRACT: Two d-4f complexes $[Zn_2NdL_2(OAc)_2]\cdot OH$ (**1**) and $[Cd_3Sm_3L_3(OAc)_6(OH)_3]$ (**2**) with a designed Schiff base ligand *N*,*N*′-bis(3-methoxysalicylidene)(binaphthyl)-1,4-diamine (H_2L) were synthesized. The Schiff base ligands coordinate with metal ions by $\mu_2(\eta^1{:}\eta^2{:}\eta^1{:}\eta^1{:}\eta^2{:}\eta^1)$ and $\mu_2(\eta^1{:}\eta^2{:}\eta^1{:}\eta^1{:}\eta^2{:}\eta^1)$ modes in the complexes, which show typical lanthanide emissions. The triangular Cd−Sm complex **2** shows both visible and NIR luminescent responses to nitrobenzene explosive 2,4,6-trinitrophenol (PA).

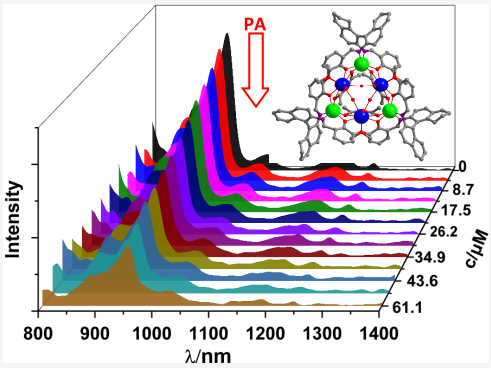

INTRODUCTION

In recent years, the application of fluorescent probes in the detection of various analytes has been a topic of intense research activity due to fast response, high sensitivities, and convenient utilization.[1−6] Explosives such as nitroaromatics have been used in many fields such as mining and military. Fluorescence-based chemical sensors for the detection of explosives have attracted much attention since they have potential applications in national security and environmental protection.[7−9] For the fluorescence-based detection, some factors (e.g., the concentrations of analytes and the power of the light source) may disturb the emission intensities of sensors. To address this deficiency, some fluorescent organic compounds,[10,11] nanoparticles,[12,13] and metal complexes[14,15] were employed as dual-emissive sensors, which can calibrate the fluorescence signals by themselves and make the results more accurate. Recently, Chi et al. first used an Eu-MOF containing carbon-based dots (CDs) to detect H_2O molecules in organic solvents, where the red light of Eu(III) and the blue emission of CDs display sensing behavior to H_2O molecules.[16] In heterometallic d-4f complexes, light-absorbing moieties with d-block metals (e.g., Zn^{2+},[17] Cd^{2+},[18] Pt^{2+},[19] Ru^{2+},[20] and Cr^{2+}[21]) may efficiently transfer energy to lanthanide ions. The dual-emissive detection based on d-4f complexes is achieved mainly so far by the intensity changes of visible emission of d-block metal chromophores and luminescence of Ln^{3+} ions.[22−24] Some lanthanide ions (e.g., Sm(III) and Ho(III)) have rich spectroscopic properties and can show visible and NIR emissions. However, as we know that there have been very few reports on dual-emissive sensors based on both visible and NIR lanthanide emissions.

Currently, our research interest has focused on the design of luminescent lanthanide-based complexes with Schiff base ligands.[25] For example, the flexible Schiff base ligands with $-CH_2-CH_2-$ backbones tended to form 30- and 32-nuclear d-4f complexes,[26−28] while the employ of conjugated salen-type Schiff base ligands such as those with phenylene backbones gave various "multidecker" lanthanide-based complexes.[29−31] Recently, we reported a Sm(III) coordination polymer with a dual-emissive response to metal ions.[32] The formation of lanthanide Schiff base complexes is usually affected by some factors, for example, the coordination modes of ligands and the types of metal ions and anions. As part of our studies, we report here the results of employing a designed ligand *N*,*N*′-bis(3-methoxysalicylidene)(binaphthyl)-1,4-diamine with a binaphthyl backbone (H_2L, Scheme 1). The purposes of the introduction of a binaphthyl ring into the Schiff base ligand are that first, a naphthyl ring has a high molar absorption coefficient, which helps to absorb and transfer more light energy for lanthanide emission, and second, the large conjugated aromatic ring can interact with aromatic compounds (e.g., nitrobenzene explosives) by intermolecular $\pi\cdots\pi$ interaction. The reactions of the Schiff base ligand with lanthanide acetates and $ZnCl_2/Cd(NO_3)_2\cdot 4H_2O$ gave d-4f complexes $[Zn_2NdL_2(OAc)_2]\cdot OH$ (**1**) and

Received: October 29, 2020
Revised: December 17, 2020
Published: January 4, 2021

https://dx.doi.org/10.1021/acs.jpca.0c09758
J. Phys. Chem. A 2021, 125, 251−257

Scheme 1. Structure Diagram of the Designed Schiff Base Ligand

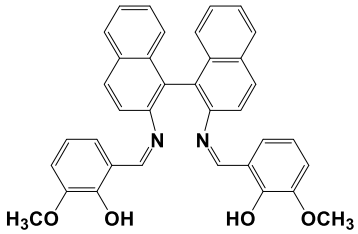

$[Cd_3Sm_3L_3(OAc)_6(OH)_3]$ (**2**). The Cd−Sm complex **2** shows a triangular structure with 12 electron-rich groups such as naphthyl and phenyl rings from H_2L, which is beneficial to forming $\pi\cdots\pi$ interactions with aromatic compounds. Interestingly, **2** exhibits both visible and NIR lanthanide luminescent responses to nitrobenzene explosives, especially to 2,4,6-trinitrophenol (PA) with high sensitivity.

■ EXPERIMENTAL SECTION

Synthesis of the Schiff Base Ligand H_2L. To a 15 mL EtOH solution of 2-hydroxy-3-methoxybenzaldehyde (20.0 mmol, 3.04 g), 1,1′-binaphthyl-2,2′-diamine (10.0 mmol, 2.84 g) in 20 mL of EtOH was added slowly in 20 min. The mixture was heated for 3.5 h under reflux with stirring. It was cooled to room temperature to give a yellow solid product, which was then filtered, washed three times using 5 mL of ethanol, and dried overnight in air. Yield: (calculated from 1,1′-binaphthyl-2,2′-diamine): 5.3607 g (97%). EA: Found: C, 78.31%; H, 5.13%; N, 5.12%. Calcd for $C_{36}H_{28}N_2O_4$: C, 78.24%; H, 5.11%; N, 5.07%. ^{1}H NMR (CD_3Cl_3, 500 MHz): 12.18 (2H), 8.46 (2H), 7.85 (4H), 7.42 (2H), 7.27 (2H), 7.09 (2H), 7.03 (2H), 6.63 (2H), 3.63 (6H). IR (KBr, cm^{-1}): 1613 (w), 1458 (m), 1251 (s), 1074 (m), 982 (s), 814 (s), 742 (s), 629 (s).

*Synthesis of $[Zn_2NdL_2(OAc)_2]\cdot OH$ (**1**).* To a 20 mL MeOH solution of $ZnCl_2$ (0.20 mmol, 0.0272 g), $Nd(OAc)_3\cdot 4H_2O$ (0.20 mmol, 0.0642 g), and H_2L (0.20 mmol, 0.1104 g), triethylamine in 1 mL of a EtOH solution (1.0 mol/L) was added. The mixture was heated for 3 h under reflux with stirring. A clear solution was obtained after filtration, and slow diffusion of ether into the solution for 2 weeks gave a yellow crystalline product of **1**. Yield (calculated from $ZnCl_2$): 0.0778 g (49%). EA: Found: C, 58.52; H, 4.51; N, 3.34%. Calcd for $C_{78}H_{66}N_4NdO_{17}Zn_2$: C, 58.32; H, 4.14; N, 3.49%. IR (KBr, cm^{-1}): 1616 (s), 1543 (s), 1436 (s), 1233 (s), 1195 (s), 1075 (m), 972 (s), 701 (s), 659 (s). mp > 179.85 °C (decompose).

*Synthesis of $[Cd_3Sm_3L_3(OAc)_6(OH)_3]$ (**2**).* The synthesis process of **2** was the same as that of **1** with the use of $Cd(NO_3)_2\cdot 4H_2O$ (0.20 mmol, 0.0472 g), $Sm(OAc)_3\cdot 6H_2O$ (0.20 mmol, 0.0654 g), and H_2L (0.20 mmol, 0.1104 g). Yield: 0.0713 g (35%). EA: Found: C, 49.51; H, 3.76; N, 2.87%. Calcd for $C_{123}H_{111}Cd_3N_6O_{31}Sm_3$: C, 49.95; H, 3.78; N, 2.84%. IR (KBr, cm^{-1}): 1609 (s), 1386 (s), 1212 (m), 1071 (m), 966 (m), 748 (w), 624 (m). mp > 172.83 °C (decompose).

X-ray Single Crystal Diffraction. A Smart APEX CCD diffractometer (Mo Kα radiation) was employed for the collection of X-ray data of the single crystals. The crystal structures of **1** and **2** have been solved by SHELX 97 program using a direct method.[33] SADABS program was used for the empirical absorption correction. Non-hydrogen atoms were refined anisotropically and located from trial structures, and hydrogen atoms were calculated by geometrical methods and refined isotropically. For **1** and **2**, their CCDC numbers of crystal structures are 2031776 and 2031777, respectively (see www.ccdc.cam.ac.uk/data_request/cif). The bond lengths and angles selected are displayed in Tables S1 and S2 (SI).

For **1**: $C_{78}H_{66}N_4O_{17}Zn_2Nd$, monoclinic ($Cc$), a = 33.516(8), b = 14.576(3), c = 17.164(4) Å, α = 90°, β = 109.594(4)°, γ = 90°, V = 7900(3) Å^3, Dc = 1.351 g cm^{-3}, Z = 4, μ(Mo Kα) = 1.316 mm^{-1}, T = 190 K, F(000) = 3372. R_1 = 0.0721, wR_2 = 0.2138, GOF = 1.009.

For **2**: $C_{123}H_{111}Cd_3N_6O_{31}Sm_3$, hexagonal ($R3$), a = 19.273(3), b = 19.273(3), c = 31.065(11) Å, α = 90°, β = 90°, γ = 120°, V = 9993(4) Å^3, Dc = 1.474 g cm^{-3}, Z = 3, μ(Mo Kα) = 1.842 mm^{-1}, T = 190 K, F(000) = 4407. R_1 = 0.0867, wR_2 = 0.1875, GOF = 1.144.

■ RESULTS AND DISCUSSION

Synthesis and Characterization. According to well-established procedures,[34] H_2L was obtained from the condensation reaction of 1,1′-binaphthyl-2,2′-diamine and 2-hydroxy-3-methoxybenzaldehyde (Figure S1), with a yield of 97%. The yellow crystalline solid of **1** was achieved by the reaction of the Schiff base ligand with $ZnCl_2$ and $Nd(OAc)_3\cdot 4H_2O$ in a EtOH/MeOH solution. As shown in Figure 1, two

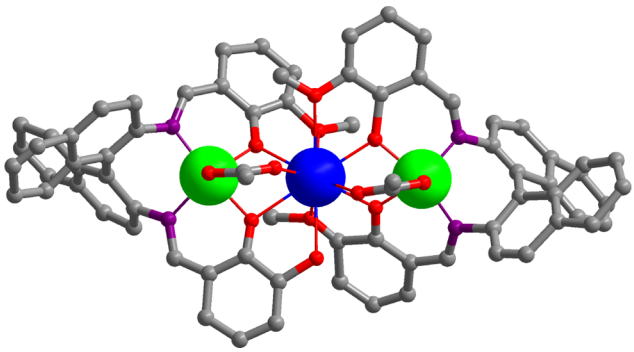

Figure 1. Structure of the trinuclear Zn−Nd complex **1** (Zn^{2+}: green; Nd^{3+}: blue).

Zn(II) ions have a square-based pyramidal geometry, located in the inner N_2O_2 cavities of two L^{2-} ligands. The Nd(III) ion is ten-coordinated and shows a coordination geometry of bicapped tetragonal antiprism, bound to the O_2O_2 donor sets of two L^{2-} ligands. The Nd(III) and Zn(II) ions are linked together through two OAc^- anions and four phenolic oxygen atoms of the L^{2-} ligands. The average Zn(II)···Nd(III) distance is 3.542 Å. In **1**, each Schiff base ligand coordinates with one Zn(II) and one Nd(III) and displays a coordination mode of $\mu_2(\eta^1{:}\eta^2{:}\eta^1{:}\eta^1{:}\eta^2{:}\eta^1)$, while the OAc^- anion exhibits a μ_2 coordination mode with the metals. The bond lengths of Nd−O, Zn−N, and Zn−O in the structures are 2.400−2.880, 1.980−2.130, and 1.980−2.080 Å, respectively.

The formation of d-4f complexes depends on the d-metal ions used, and the reaction of Schiff base ligand with $Sm(OAc)_3\cdot 6H_2O$ and $Cd(NO_3)_2\cdot 4H_2O$ gave **2** under the same experimental conditions as above. The hexanuclear Cd−Sm complex **2** shows an interesting triangular structure, which has a C_3 symmetry axis through the center of the molecule (Figure 2). Different from those in **1**, two benzene rings of the L^{2-} ligand are more distorted in **2**. Thus, the L^{2-} ligand can coordinate with three metal ions (one Cd(II) and two Sm(III)), resulting in a coordination mode of

https://dx.doi.org/10.1021/acs.jpca.0c09758
J. Phys. Chem. A 2021, 125, 251−257

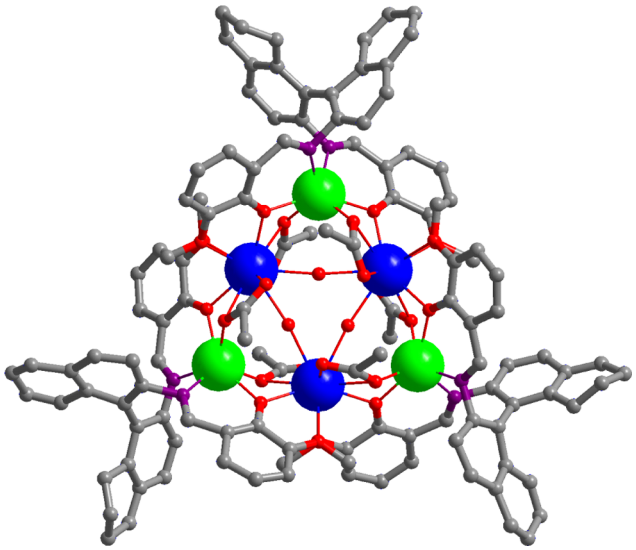

Figure 2. Triangular structure of the hexanuclear Cd−Sm complex **2** (Cd^{2+}: green; Sm^{3+}: blue).

$\mu_3(\eta^1{:}\eta^2{:}\eta^1{:}\eta^1{:}\eta^2{:}\eta^1)$. The Cd(II) ions are bound to the O_2O_2 donor sets of Schiff base ligands, while the Sm(III) ions are coordinated with the O atoms of L^{2-} ligands. The Sm(III) ions are nine-coordinated and show a distorted tricapped trigonal prism geometry. All Cd(II) and Sm(III) ions are connected through three μ_3-L^{2-} ligands, three μ_2-OH^-, and six μ_2-OAc^- anions. The average Cd(II)···Sm(III) distance is 3.759 Å, and the bond lengths of Sm−O, Cd−N, and Cd−O are 2.370−2.871, 2.269−2.363, and 2.240−2.339 Å, respectively. In Figure 3, an image of scanning electron microscopy (SEM)

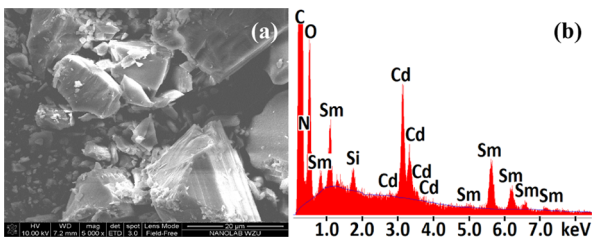

Figure 3. SEM image (a) and EDX spectroscopy (b) of **2**.

exhibits the crystalline nature of **2**, and the molar ratio of Cd/Sm in its energy-dispersive X-ray spectroscopy (EDX) is found to be 1, consistent with the crystal structure. For **1** and **2**, their power XRD spectra are similar to those generated from their crystal data (Figure S3). Melting point measurements and thermogravimetric analyses show that **1** and **2** are stable before 170 °C (see Experimental Section and Figure S4).

Photophysical Properties. The emission and excitation spectra of the lanthanide complexes were investigated in CH_3CN. The free H_2L displays UV−vis absorption bands at 233, 285, and 319 nm, which are all shifted in **1** and **2** (Figure 4). Under excitation at 373 nm, the H_2L ligand has an emission band at 621 nm (Figure S5). As shown in Figures 5 and 6, the typical Nd(III) luminescence of **1** (NIR: $^4F_{3/2} \rightarrow {}^4I_{j/2}$ transitions, j = 9, 11, and 13) and Sm(III) emissions of **2** (visible: $^4G_{5/2} \rightarrow {}^6H_{j/2}$ transitions, j = 5, 7, 9, and 11; NIR: $^4G_{5/2} \rightarrow {}^6F_{j/2}$ transitions, j = 1, 3, 5, 7, and 9) are detected upon excitations at the absorption bands of ligands, indicating that the energy transfer from Schiff base ligands to lanthanide

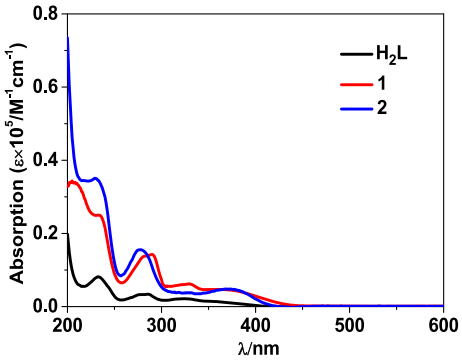

Figure 4. Absorption bands of the Schiff base ligand, **1**, and **2** in CH_3CN.

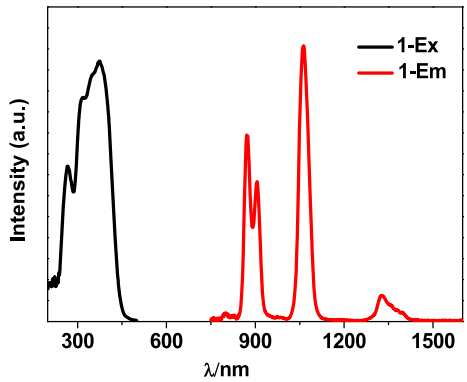

Figure 5. Lanthanide luminescence of **1** in CH_3CN (C = 40 μM).

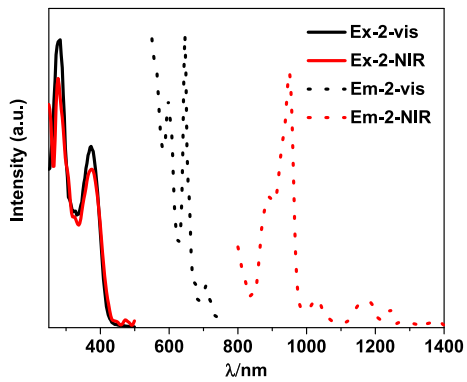

Figure 6. Lanthanide luminescence of **2** in CH_3CN (C = 5 μM).

ions (LMET) happens in the complexes.[35] The fluorescence data of the free Schiff base ligand and complexes can be found in Table 1.

Sensing Behavior of Complexes to Explosives. The luminescence sensing behavior of **1** and **2** to nitrobenzene

Table 1. Fluorescence Data of the Free H_2L and Complexes 1 and 2

	λ_{ex} (nm)/ε ($\times 10^5$ $M^{-1}cm^{-1}$)	λ_{em} (nm)	τ (μs)	Φ_{em} (%)
H_2L	373/0.01	621		
1	374/0.045	871, 906, 1063, 1327	5.81	0.32
2	Vis: 283/0.15, 373/0.05	598, 646, 709	16.57	
	NIR: 277/0.16, 373/0.05	899, 950, 1028, 1178, 1244	7.64	0.12

https://dx.doi.org/10.1021/acs.jpca.0c09758
J. Phys. Chem. A 2021, 125, 251−257

explosives (Scheme S1) was investigated in CH_3CN. The NIR luminescence of **1** can be quenched by the addition of explosives. As shown in Figure 7, with the addition of 60 μM

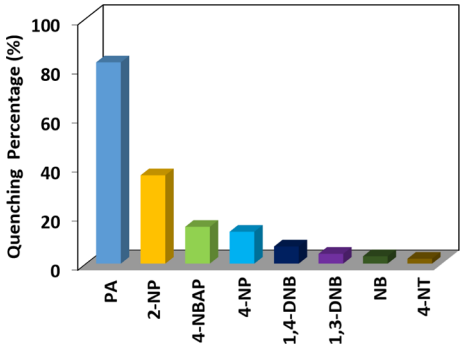

Figure 7. Quenching percentages of the lanthanide emission of **1** (40 μM) to the addition of 60 μM explosives in CH_3CN.

PA, the luminescence quenching percentage of **1** is 82%, which is much higher than those caused by the addition of other explosives with the same concentration (less than 40%). It is noticeable that the added explosives can decrease the lanthanide luminescence of **2** in either visible or NIR range (Figures 8,9, S7, and S8), indicating that **2** shows dual

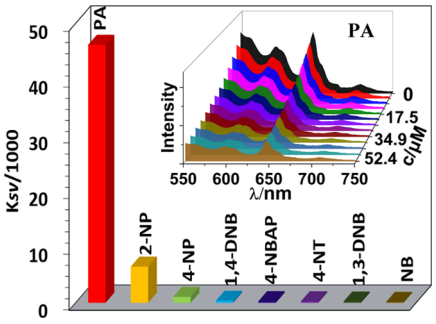

Figure 8. K_{sv} values of **2** to explosives for the visible luminescence quenching. The inset shows the visible emission quenching of **2** (5 μM) to the addition of PA.

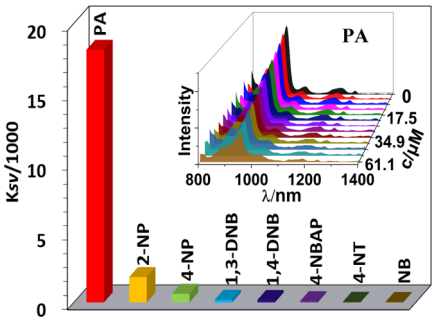

Figure 9. K_{sv} values of **2** to explosives for the NIR luminescence quenching. The inset shows the NIR emission quenching of **2** (50 μM) to the addition of PA.

luminescent response properties to explosives. Compared with other explosives, the low concentration of PA can quench the luminescence rapidly. For example, the most intense lanthanide emissions of **2** at 646 and 950 nm are decreased about a half, with the addition of 21.8 and 39.3 μM PA, respectively (Figures S7 and S8). These two concentrations are much lower compared to those required for other explosives, demonstrating the high sensitivity of **2** to PA by both visible and NIR luminescent responses.

The luminescence quenching is linear with the increase of the concentrations of explosives (Figures S7 and S8). Thus, the visible (or NIR) luminescence quenching constants (K_{sv}) of **2** to explosives can be estimated by the Stern−Volmer equation $I_o/I = 1 + K_{sv}[A]$,[36] in which I_o and I are the luminescence intensities at 646 nm (or 950 nm) in the absence and presence of the explosive, respectively, and $[A]$ represents its added concentration (M) (Figures 8 and 9). For **2**, the quenching constants of visible and NIR luminescent responses to PA are 4.62×10^4 and 1.81×10^4 M^{-1}, respectively, which are among the highest values so far reported for the fluorescent detection of explosives.[37−40] The limits of detection (LOD = $3\sigma/K_{sv}$[41]) of **2** to PA by the visible and NIR luminescent responses are estimated to be 1.1×10^{-6} and 2.1×10^{-5} M, respectively. These results demonstrate that **2** exhibits visible and NIR luminescence sensing to PA with high sensitivity.

The stability of **2** during the response experiments is checked by powder X-ray diffraction (PXRD). The PXRD pattern of **2** after treated with PA is similar to that treated before, indicating that the structure of the Cd(II)−Sm(III) complex is not changed during the experiments (Figure S9). Thus, the luminescence quenching of **2** with the addition of PA is not due to the decomposition of the complex or the coordination of PA with Sm(III) ions in **2**. For luminescent lanthanide complexes, the organic ligands are able to absorb and transfer light energy to Ln(III) ions ("antenna effect").[42,43] Thus, if the added explosives have high molar absorption coefficients at the λ_{ex} of **2**, they may quench lanthanide luminescence by the "inner filter effect" (Scheme 2).[44] As

Scheme 2. "Antenna Effect" of Schiff Base Ligands and the "Inner Filter Effect" of Explosives to the Lanthanide Luminescence of 2

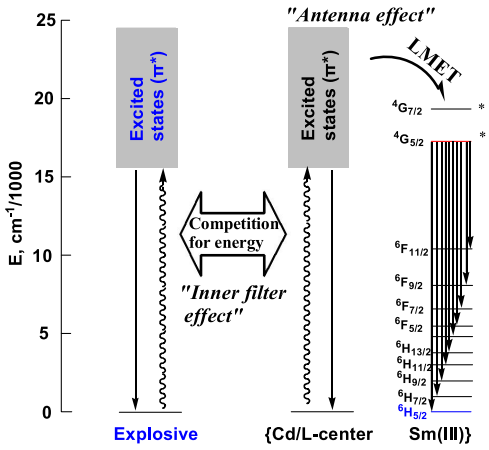

shown in Figure 10, the absorption coefficient of PA at λ_{ex} = 373 nm is 1.6×10^4 M^{-1} cm^{-1}, which is higher than that of **2** at the excitation wavelength (0.5×10^4 M^{-1} cm^{-1}; Table 1). Thus, the added PA can compete for the light energy with the Schiff base ligands in **2**, resulting in the lanthanide emission quenching of the complex. In addition, the absorption coefficient of 2-NP at 373 nm is found to be 0.2×10^4 M^{-1} cm^{-1}, which is lower than that of PA but much higher than those of other explosives that almost show no absorption at this wavelength (Figure 10). As a result, **2** has the second

https://dx.doi.org/10.1021/acs.jpca.0c09758
J. Phys. Chem. A 2021, 125, 251−257

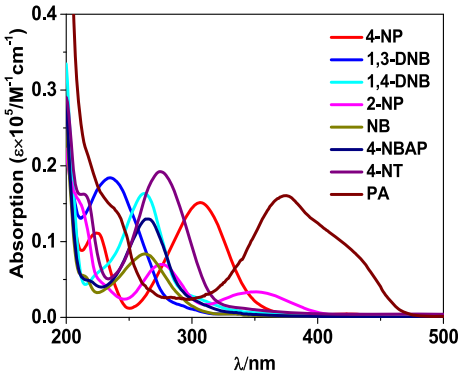

Figure 10. UV−vis spectra of nitrobenzene explosives in CH_3CN at room temperature.

highest visible and NIR luminescence quenching constants to 2-NP (0.65×10^4 and 0.18×10^4 M^{-1}; Figures 8 and 9), confirming the inner filter effect of explosives to the lanthanide emission quenching.

For the visible (or NIR) luminescence of **2**, besides the excitation wavelength at 373 nm, another excitation wavelength is at 283 nm (or 277 nm), where the absorption coefficient of PA is 0.27×10^4 M^{-1} cm^{-1} (or 0.26×10^4 M^{-1} cm^{-1}). The absorption coefficients of **2** at 277 and 283 nm are 1.6×10^4 and 1.5×10^4 M^{-1} cm^{-1}, respectively, which are higher than those of PA at these two excitation wavelengths. When the excitation wavelengths of the visible and NIR luminescence are changed to 283 and 277 nm, the K_{sv} values of **2** to PA are 0.82×10^4 and 0.77×10^4 M^{-1}, respectively (Figure S10), which are lower than those obtained with the excitation wavelength at 373 nm. This is due to the higher absorption coefficients of **2** at 283 and 277 nm. These results further demonstrate that the inner filter effect of PA plays an important role in the lanthanide emission quenching of **2**.

As shown in Figures 11 and 12, the step-by-step addition of nitrobenzene explosives has been employed to study the effect

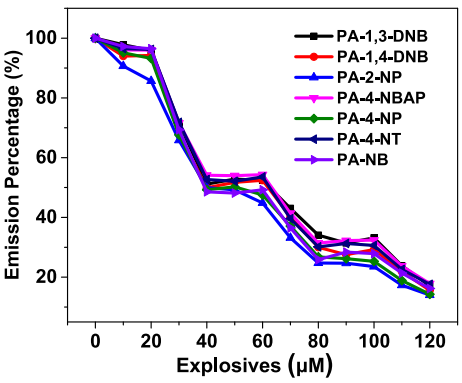

Figure 11. Visible lanthanide emission quenching of **2** (5 μM) in CH_3CN caused by the step-by-step addition of nitrobenzene explosives (10 μM).

of other explosives on the emission sensing of **2** to PA. The emission quenching of **2** to PA and other explosives shows that the visible (or NIR) luminescence was not reduced rapidly when another explosive such as 1,3-DNB was added twice first, while it was decreased much fast with the subsequent addition of PA. This phenomenon can be found again in the following

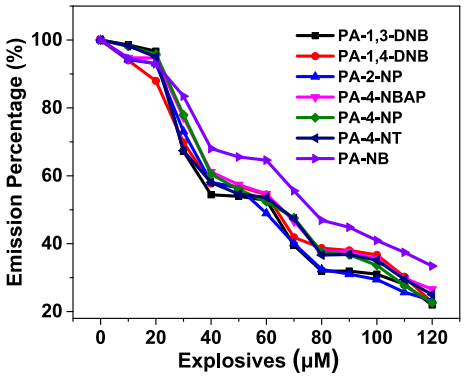

Figure 12. NIR lanthanide emission quenching of **2** (50 μM) in CH_3CN caused by the step-by-step addition of explosives (10 μM).

cycles of the additions of another explosive and PA, suggesting the high selectivity of **2** to the latter.

■ CONCLUSIONS

In brief, two Zn−Nd and Cd−Sm complexes **1** and **2** were synthesized from a designed Schiff base ligand H_2L that has a binaphthyl backbone and coordinates with metal ions by $\mu_2(\eta^1{:}\eta^2{:}\eta^1{:}\eta^1{:}\eta^2{:}\eta^1)$ and $\mu_2(\eta^1{:}\eta^2{:}\eta^1{:}\eta^1{:}\eta^2{:}\eta^1)$ modes. The Schiff base ligands can transfer light energy to lanthanide ions, resulting in the typical Nd(III) and Sm(III) emissions of the complexes. The triangular Cd−Sm complex **2** exhibits interesting dual visible and NIR emissive responses to nitrobenzene explosives and shows high sensitivity and selectivity to PA. The quenching constants to PA for the visible and NIR lanthanide emissions of **2** are 4.62×10^4 and 1.81×10^4 M^{-1}, respectively.

■ ASSOCIATED CONTENT

Supporting Information

The Supporting Information is available free of charge at https://pubs.acs.org/doi/10.1021/acs.jpca.0c09758.

General procedures; ^{1}H NMR spectra of H_2L; IR spectra of H_2L and complexes **1** and **2**; powder XRD patterns of **1** and **2**; thermogravimetric analysis of **1** and **2**; chemical structures of nitro explosives; NIR luminescence sensing of **2** to nitro explosives; powder XRD patterns of **2** before and after treated with PA; and CCDC numbers for **1** and **2** are 2031776 and 2031777, respectively (PDF)

■ AUTHOR INFORMATION

Corresponding Author

Xiaoping Yang − *Zhejiang Key Laboratory of Carbon Materials, College of Chemistry and Materials Engineering, Wenzhou University, Wenzhou 325035, China;* orcid.org/0000-0002-4370-517X; Email: xpyang@wzu.edu.cn

Authors

Mengyu Niu − *Zhejiang Key Laboratory of Carbon Materials, College of Chemistry and Materials Engineering, Wenzhou University, Wenzhou 325035, China*

Yanan Ma − *Zhejiang Key Laboratory of Carbon Materials, College of Chemistry and Materials Engineering, Wenzhou University, Wenzhou 325035, China*

Dongliang Shi − *Zhejiang Key Laboratory of Carbon Materials, College of Chemistry and Materials Engineering, Wenzhou University, Wenzhou 325035, China*
Desmond Schipper − *Department of Chemistry and Biochemistry, The University of Texas at Austin, Austin, Texas 78712-0165, United States*

Complete contact information is available at:
https://pubs.acs.org/10.1021/acs.jpca.0c09758

Author Contributions

The manuscript was written through contributions of all authors. All authors have given approval to the final version of the manuscript.

Notes

The authors declare no competing financial interest.

■ ACKNOWLEDGMENTS

This work was supported by the National Natural Science Foundation of China (No. 21771141) and Key Foundation for High-level Talents Innovation Technology Projects of Wenzhou (2019).

■ REFERENCES

(1) Shi, P.; Hu, H.; Zhang, Z.; Xiong, G.; Zhao, B. Heterometal−organic frameworks as highly sensitive and highly selective luminescent probes to detect I^- ions in aqueous solutions. *Chem. Commun.* **2015**, *51*, 3985−3988.
(2) Xu, Y.-Y.; Sun, O.; Xie, B.-Y.; Gao, T.; Qi, Y. Enhanced luminescence for detection of small molecules based on doped lanthanide compounds with a dinuclear double-stranded helicate structure. *New J. Chem.* **2019**, *43*, 16706−16713.
(3) Guo, Z.; Xu, H.; Su, S.; Cai, J.; Dang, S.; Xiang, S.; Qian, G.; Zhang, H.; O'Keeffe, M.; Chen, B. A robust near infrared luminescent ytterbium metal-organic framework for sensing of small molecules. *Chem. Commun.* **2011**, *47*, 5551−5553.
(4) Hou, S.-L.; Dong, J.; Tang, M.-H.; Jiang, X.-L.; Jiao, Z.-H.; Zhao, B. Triple-interpenetrated lanthanide-organic framework as dual wave bands self-calibrated pH luminescent probe. *Anal. Chem.* **2019**, *91*, 5455−5460.
(5) Kang, X.-M.; Fan, X.-Y.; Hao, P.-Y.; Wang, W.-M.; Zhao, B. A stable zinc-organic framework with luminescence detection of acetylacetone in aqueous solution. *Inorg. Chem. Front.* **2019**, *6*, 271−277.
(6) Kang, X.-M.; Hu, H.-S.; Wu, Z.-L.; Wang, J.-Q.; Cheng, P.; Li, J.; Zhao, B. An ultrastable matryoshka $[HF_{13}]$ nanocluster as a luminescent sensor for concentrated alkali and acid. *Angew. Chem., Int. Ed.* **2019**, *58*, 16610−16616.
(7) Qi, X.; Jin, Y.; Li, N.; Wang, Z.; Wang, K.; Zhang, Q. A luminescent heterometallic metal−organic framework for the naked-eye discrimination of nitroaromatic explosives. *Chem. Commun.* **2017**, *53*, 10318−10321.
(8) Sun, X.; Wang, Y.; lei, Y. Fluorescence based explosive detection: from mechanisms to sensory materials. *Chem. Soc. Rev.* **2015**, *44*, 8019−8061.
(9) Hu, Z.; Deibert, B. J.; Li, J. Luminescent metal−organic frameworks for chemical sensing and explosive detection. *Chem. Soc. Rev.* **2014**, *43*, 5815−5840.
(10) Takahashi, S.; Piao, W.; Matsumura, Y.; Komatsu, T.; Ueno, T.; Terai, T.; Kamachi, T.; Kohno, M.; Nagano, T.; Hanaoka, K. Reversible off−On fluorescence probe for hypoxia and imaging of hypoxia−normoxia cycles in live cells. *J. Am. Chem. Soc.* **2012**, *134*, 19588−19591.
(11) Huang, C.; Jia, T.; Tang, M.; Yin, Q.; Zhu, W.; Zhang, C.; Yang, Y.; Jia, N.; Xu, Y.; Qian, X. Selective and ratiometric fluorescent trapping and quantification of protein vicinal dithiols and in situ dynamic tracing in living cells. *J. Am. Chem. Soc.* **2014**, *136*, 14237−14244.
(12) Ma, H.; Song, B.; Wang, Y.; Cong, D.; Jiang, Y.; Yuan, J. Dual-emissive nanoarchitecture of lanthanide-complex-modified silica particles for in vivo ratiometric time-gated luminescence imaging of hypochlorous acid. *Chem. Sci.* **2017**, *8*, 150−159.
(13) Zhang, K. Y.; Zhang, J.; Liu, Y.; Liu, S.; Zhang, P.; Zhao, Q.; Tang, Y.; Huang, W. Core−shell structured phosphorescent nanoparticles for detection of exogenous and endogenous hypochlorite in live cells via ratiometric imaging and photoluminescence lifetime imaging microscopy. *Chem. Sci.* **2015**, *6*, 301−307.
(14) Zhang, K. Y.; Liu, H.; Tang, M.; Choi, A. W.; Zhu, N.; Wei, X.; Lau, K.; Lo, K. K. Dual-emissive cyclometalated Iridium(III) polypyridine complexes as ratiometric biological probes and organelle-selective bioimaging reagents. *Inorg. Chem.* **2015**, *54*, 6582−6593.
(15) Yoshihara, T.; Yamaguchi, Y.; Hosaka, M.; Takeuchi, T.; Tobita, S. Ratiometric molecular sensor for monitoring oxygen levels in living cells. *Angew. Chem., Int. Ed.* **2012**, *51*, 4148−4151.
(16) Dong, Y.; Cai, J.; Fang, Q.; You, X.; Chi, Y. Dual-emission of lanthanide metal−organic frameworks encapsulating carbon-based dots for ratiometric detection of water in organic solvents. *Anal. Chem.* **2016**, *88*, 1748−1752.
(17) Wong, W.-K.; Liang, H.; Wong, W.-Y.; Cai, Z.; Li, K.-F.; Cheah, K.-W. Synthesis and near-infrared luminescence of 3d-4f bi-metallic Schiff base complexes. *New J. Chem.* **2002**, *26*, 275−278.
(18) Chi, Y.-X.; Niu, S.-Y.; Jin, J.; Wang, R.; Li, Y. Syntheses, structures and photophysical properties of tetranuclear Cd−Ln coordination complexes. *Dalton Trans.* **2009**, 7653−7659.
(19) Xu, H.-B.; Shi, L.-X.; Ma, E.; Zhang, L.-Y.; Wei, Q.-H.; Chen, Z.-N. Diplatinum alkynyl chromophores as sensitisers for lanthanide luminescence in Pt_2Ln_2 and Pt_2Ln_4 (Ln = Eu, Nd, Yb) arrays with acetylide-functionalized bipyridine/phenanthroline. *Chem. Commun.* **2006**, 1601−1603.
(20) Baca, S. G.; Adams, H.; Grange, C. S.; Smith, A. P.; Sazanovich, I.; Ward, M. D. $[Os(bipy)(CN)_4]^{2-}$ and Its relatives as components of polynuclear assemblies: Structural and photophysical properties. *Inorg. Chem.* **2007**, *46*, 9779−9789.
(21) Torelli, S.; Imbert, D.; Cantuel, M.; Bernardinelli, G.; Delahaye, S.; Hauser, A.; Bünzli, J.-C. G.; Piguet, C. Tuning the decay time of lanthanide-based near infrared luminescence from micro- to milliseconds through d→f energy transfer in discrete heterobimetallic complexes. *Chem. - Eur. J.* **2005**, *11*, 3228−3242.
(22) Boulay, A.; Deraeve, C.; Elst, L. V.; Leygue, N.; Maury, O.; Laurent, S.; Muller, R. N.; Mestre-Voegtlé, B.; Picard, C. Terpyridine-based heteroditopic ligand for $Ru^{II}Ln_3^{III}$ metallostar architectures (Ln = Gd, Eu, Nd, Yb) with MRI/optical or dual-optical responses. *Inorg. Chem.* **2015**, *54*, 1414−1425.
(23) Nonat, A. M.; Quinn, S. J.; Gunnlaugsson, T. Mixed f−d coordination complexes as dual visible- and near-Infrared-emitting probes for targeting DNA. *Inorg. Chem.* **2009**, *48*, 4646−4648.
(24) Comby, S.; Tuck, S. A.; Truman, L. K.; Kotova, O.; Gunnlaugsson, T. New trick for an old ligand! the sensing of Zn(II) using a lanthanide based ternary Yb(III)-cyclen-8-hydroxyquinoline system as a dual emissive probe for displacement assay. *Inorg. Chem.* **2012**, *51*, 10158−10168.
(25) Yang, X.; Jones, R. A.; Huang, S. Luminescent 4f and d-4f polynuclear complexes and coordination polymers with flexible salen-type ligands. *Coord. Chem. Rev.* **2014**, *273−274*, 63−75.
(26) Yang, X.; Schipper, D.; Jones, R. A.; Lytwak, L. A.; Holliday, B. J.; Huang, S.-M. Anion dependent self-Assembly of NIR luminescent 24- and 32-metal Cd-Ln complexes with drum-like architectures. *J. Am. Chem. Soc.* **2013**, *135*, 8468−8471.
(27) Yang, X.; Schipper, D.; Zhang, L.; Yang, K.; Huang, S.; Jiang, J.; Su, C.; Jones, R. A. Anion dependent self-assembly of 56-metal Cd-Ln nanoclusters with enhanced near-infrared luminescence properties. *Nanoscale* **2014**, *6*, 10569−10573.
(28) Wang, C.; Yang, X.; Wang, S.; Zhu, T.; Bo, L.; Zhang, L.; Chen, H.; Jiang, D.; Dong, X.; Huang, S. Anion dependent self-assembly of

drum-like 30- and 32-metal Cd-Ln nanoclusters: visible and NIR luminescent sensing of metal cations. *J. Mater. Chem. C* **2018**, *6*, 865−874.

(29) Yang, X.; Jones, R. A. Anion dependent self-assembly of "tetra-decker" and "triple-decker" luminescent Tb(III) salen complexes. *J. Am. Chem. Soc.* **2005**, *127*, 7686−7689.

(30) Yang, X.; Jones, R. A.; Wong, W.-K. Pentanuclear tetra-decker luminescent lanthanide Schiff base complexes. *Dalton Trans.* **2008**, 1676−1678.

(31) Wong, W. K.; Yang, X.; Jones, R. A.; Rivers, J.; Lynch, V.; Lo, W. K.; Xiao, D.; Oye, M. M.; Holmes, A. Multinuclear luminescent Schiff-base Zn-Nd sandwich complexes. *Inorg. Chem.* **2006**, *45*, 4340−4345.

(32) Liu, J.; Zhu, T.; Yang, X.; Chen, H.; Shi, D.; Zhu, C.; Schipper, D.; Jones, R. A. Construction of a 1-D Sm(III) coordination polymer with long-chain Schiff base ligand: Dual-emissive response to metal ions. *Inorg. Chem. Front.* **2020**, *7*, 464−469.

(33) Sheldrick, G. H. *SHELX 97, A Software Package for the Solution and Refinement of X-ray Data*; University of Göttingen: Göttingen, Germany, 1997.

(34) Lam, F.; Xu, J. X.; Chan, K. S. Binucleating ligands: synthesis of acyclic achiral and chiral Schiff base-pyridine and Schiff base-phosphine ligands. *J. Org. Chem.* **1996**, *61*, 8414−8418.

(35) Petoud, S.; Cohen, S. M.; Bünzl, J.-C. G.; Raymond, K. N. Stable lanthanide luminescence agents highly emissive in aqueous solution: Multidentate 2-hydroxyisophthalamide complexes of Sm^{3+}, Eu^{3+}, Tb^{3+}, Dy^{3+}. *J. Am. Chem. Soc.* **2003**, *125*, 13324−13325.

(36) Xiao, Y.; Cui, Y.; Zheng, Q.; Xiang, S.; Qian, G.; Chen, B. A microporous luminescent metal−organic framework for highly selective and sensitive sensing of Cu^{2+} in aqueous solution. *Chem. Commun.* **2010**, *46*, 5503−5505.

(37) Liu, C.; Zhou, L.; Tripathy, D.; Sun, Q. Self-assembly of stable luminescent lanthanide supramolecular M_4L_6 cages with sensing properties toward nitroaromatics. *Chem. Commun.* **2017**, *53*, 2459−2462.

(38) Nagarkar, S. S.; Joarder, B.; Chaudhari, A. K.; Mukherjee, S.; Ghosh, S. K. Highly selective detection of nitro explosives by a luminescent metal-organic framework. *Angew. Chem., Int. Ed.* **2013**, *52*, 2881−2885.

(39) Nagarkar, S. S.; Desai, A. V.; Ghosh, S. K. A fluorescent metal−organic framework for highly selective detection of nitro explosives in the aqueous phase. *Chem. Commun.* **2014**, *50*, 8915−8918.

(40) Qin, J.-H.; Ma, B.; Liu, X.-F.; Lu, H.-L.; Dong, X.-Y.; Zang, S.-Q.; Hou, H.-W. Aqueous- and vapor-phase detection of nitroaromatic explosives by a water-stable fluorescent microporous MOF directed by an ionic liquid. *J. Mater. Chem. A* **2015**, *3*, 12690−12697.

(41) Qi, X.; Jin, Y.; Li, N.; Wang, Z.; Wang, K.; Zhang, Q. A luminescent heterometallic metal-organic framework for the naked-eye discrimination of nitroaromatic explosives. *Chem. Commun.* **2017**, *53*, 10318−10321.

(42) Sabbatini, N.; Guardigli, M.; Lehn, J. M. Luminescent lanthanide complexes as photochemical supramolecular devices. *Coord. Chem. Rev.* **1993**, *123*, 201−228.

(43) Piguet, C.; Bünzli, J.-C. G. Mono- and polymetallic lanthanide-containing functional assemblies: a field between tradition and novelty. *Chem. Soc. Rev.* **1999**, *28*, 347−358.

(44) Tian, D.; Li, Y.; Chen, R. Y.; Chang, Z.; Wang, G. Y.; Bu, X. H. A luminescent metal−organic framework demonstrating ideal detection ability for nitroaromatic explosives. *J. Mater. Chem. A* **2014**, *2*, 1465−1470.

https://dx.doi.org/10.1021/acs.jpca.0c09758
J. Phys. Chem. A 2021, 125, 251−257